An Efficient Framework For Fast Computer Aided Design of Microwave Circuits Based on the Higher-Order 3D Finite-Element Method (Invited Paper)

Adam LAMECKI, Lukasz BALEWSKI, Michal MROZOWSKI

Dept. of Microwave and Antenna Engineering, Gdańsk University of Technology
Narutowicza 11/12, 80-233 Gdańsk, Poland

adlam@ieee.org, lukasz.balewski@gmail.com, m.mrozowski@ieee.org

Abstract. *In this paper, an efficient computational framework for the full-wave design by optimization of complex microwave passive devices, such as antennas, filters, and multiplexers, is described. The framework consists of a computational engine, a 3D object modeler, and a graphical user interface. The computational engine, which is based on a finite element method with curvilinear higher-order tetrahedral elements, is coupled with built-in or external gradient-based optimization procedures. For speed, a model order reduction technique is used and the gradient computation is achieved by perturbation with geometry deformation, processed on the level of the individual mesh nodes. To maximize performance, the framework is targeted to multicore CPU architectures and its extended version can also use multiple GPUs. To illustrate the accuracy and high efficiency of the framework, we provide examples of simulations of a dielectric resonator antenna and full-wave design by optimization of two diplexers involving tens of unknowns, and show that the design can be completed within the duration of a few simulations using industry-standard FEM solvers. The accuracy of the design is confirmed by measurements.*

Keywords

FEM, computational electromagnetics, microwave filters, multiplexer design, CAD, electromagnetic optimization.

1. Introduction

Computer aided design CAD combines simulation with optimization, and as such involves extensive simulation. Because of the distributed character of microwave circuits and the fact that full-wave simulations are time consuming, microwave CAD is usually associated with techniques based on simplified equivalents, surrogate models, or fast numerical methods whose applicability is limited to specific geometries. When it comes to the design of passive structures of arbitrary shape, possibly loaded with inhomogeneous material, design by optimization becomes extremely time consuming. This is because the full-wave techniques suitable for solving the underlying Maxwell's equation are numerically expensive. If the number of design variables is small, a direct full-wave optimization may be successful, but as the complexity of the circuit grows and the number of the design variables increases, the use of direct optimization with full-wave methods is considered impractical, due to the poor convergence of gradient-based techniques and the high cost of a single design iteration. To alleviate this problem, techniques such as space-mapping [13] have been devised. In space mapping, optimization is carried out with a low-cost coarse model, and the full-wave solution is used only to calibrate the coarse model. However, space-mapping requires the provision of a coarse model; such a model may not be readily available, or may unsuitable for use with gradient-based optimization techniques. On the other hand, engineers would prefer to use a single CAD tool that would yield the final design, rather than having to employ different software packages or develop procedures to integrate them. This situation motivated us to create a framework for fast full-wave CAD of complex microwave devices, which consists of a highly accurate and efficient computational engine combined with 3D object modeler, both integrated with gradient-based optimization procedures. At the heart of the framework is a multithreaded finite element method solver based on higher-order curvilinear tetrahedral elements and a fast frequency sweep technique that uses the model order reduction concept. This solver and the optimization procedures are coupled to the solid object modeler to evaluate the mesh perturbation and to quickly compute high-quality gradients.

2. Computational Engine

To perform a full-wave analysis of a 3-dimensional problem occurring in microwave passive component design,

it is necessary to solve the vector Helmholtz equation within the desired frequency band. The problem in general involves lossy and anisotropic media. For simplicity, let us assume a lossless case with isotropic dielectrics. For this class of problems, the Helmholtz equation to be solved is

$$\nabla \times \mu^{-1} \nabla \times \boldsymbol{E} - \omega^2 \varepsilon \boldsymbol{E} = 0 \tag{1}$$

with proper boundary conditions on PEC, PMC surfaces, and excitation at ports. Any numerical technique for solving this boundary value problem (BVP) should be flexible in terms of its ability to handle irregular geometry and a variety of media. One technique that meets these criteria is the finite element method (FEM) in the frequency domain. We use this method in our design-by-optimization framework.

In the finite element method, the starting point is the weak form of (1)

$$\int_V \boldsymbol{W} \cdot \left(\nabla \times \mu^{-1} \nabla \times \boldsymbol{E} - {k_0}^2 \varepsilon_r \boldsymbol{E} \right) \mathrm{d}V = 0. \tag{2}$$

The above equation is solved in the discrete domain and converted to a system of linear equations by means of the Galerkin procedure. To this end, the computational domain is meshed and the field within each mesh element (volumes, surfaces, and edges) is represented as a linear combination of vector basis functions W. Solving this system using the Galerkin method yields the impedance parameters of the N-port device [1]:

$$Z(j\omega) = j\omega\mu_0 B^T \cdot (K - k_0^2 M)^{-1} \cdot B \tag{3}$$

where K, M are sparse matrices defined as:

$$K = \iiint_V (\nabla \times N \cdot \mu_r^{-1} \nabla \times N) \mathrm{d}V, \tag{4}$$

$$M = \iiint_V (N \cdot \varepsilon_r N) \mathrm{d}V \tag{5}$$

and N are the basis functions defined over the elements. Matrix B is constructed by taking the excitation vectors in the ports as columns. Each column vector is defined by one modal field on the port surface S with proper normalization. In the proposed approach, the set of hierarchical basis functions defined over curvilinear, second-order tetrahedral elements proposed in [2] was used.

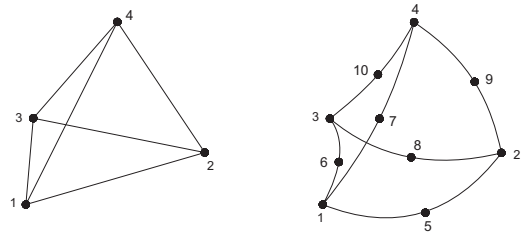

Fig. 1. Illustration of 4-node linear (a) and 10-node curvilinear (b) tetrahedral mesh elements.

This allows very good accuracy to be achieved in the geometric modeling of curved surfaces, at the same time reducing the number of mesh tetrahedra. To obtain the highest accuracy without excessive use of computer resources, we use error indicators to mark regions that require a finer mesh. The public-domain Netgen mesher [3] is used to obtain a conformal mesh. To ensure high mesh quality, the mesh is generated through an adaptive process in which error indicators are computed for each tetrahedron and the regions with the highest errors are remeshed. The process stops when the results stabilize.

The linear problem arising is defined in (3) and is large and sparse. Design of a microwave component requires several iterations of the optimization procedure. In each iteration, the response is evaluated within a frequency band of interest. If a standard discrete frequency sweep is used, the system of linear equations generated at each iteration must be solved anew at each frequency point, which leads to a high computational cost for the FEM analysis. For this reason, it is essential to apply one of the acceleration techniques often referred to as fast frequency sweep.

2.1 Fast Frequency Sweep with MOR

To obtain run-time savings, several advanced techniques for performing fast frequency sweep have been developed. One way to reduce the duration of the frequency response evaluation that is often encountered in commercial software is to use adaptive interpolation. In this approach, often called adaptive frequency sampling, a wideband response is interpolated from the results obtained for carefully selected frequency points. The points for interpolation are determined automatically [4]. As a result, the response is sampled more densely where needed. Another option to accelerate simulation within a specified frequency band is to apply a subspace projection technique. The main idea in this approach is to find a low-dimensional space in which an approximate solution to a large system of FEM equations can be found. Since the reduced problem is small, it can be efficiently solved for a high number of frequency points. There are several subspace projection algorithms, including asymptotic waveform evaluation (AWE) [5, 6], the reduced basis method (RBM) [7], and moment-matching model order reduction (MOR), which use the Krylov subspace to find the projection basis [8], [9]. Once the projection basis V has been found, the original FEM matrices are transformed to the reduced matrices in the following way:

$$\hat{K} = V^T \cdot K \cdot V, \tag{6}$$

$$\hat{M} = V^T \cdot M \cdot V, \tag{7}$$

$$\hat{B} = V^T \cdot B. \tag{8}$$

The reduced problem has the form

$$Z(j\omega) \approx \hat{Z}(j\omega) = j\omega\mu_0 \hat{B}^T \cdot (\hat{K} - k_0^2 \hat{M})^{-1} \cdot \hat{B}. \tag{9}$$

The order P of the reduced model is defined as the number vectors that span the projection basis V. For many practical problems in the CAD of passive components, the order of the model is a few orders of magnitude lower than the original order. For example, in the case of filter design, the minimum order of the reduced model may be as low as the order of the filter (or the order of highest channel filter, in the multiplexer case) times the number of ports. If one is interested in out-of-band responses, including spurious passbands, then the size of the projection basis needs to be increased, but is in any case much smaller than the size of the original system. Finally, MOR can be used in selected regions and nested to generate extremely compact reduced-order models for FEM problems that involve a large number of unknowns [18].

The reduced model can be efficiently evaluated, since computing its response $\hat{Z}(j\omega)$ involves solving a small system of linear equations.

The ideas presented here can be generalized to the lossy case with anisotropic media described by complex frequency-dependent permittivity or permeability tensors.

3. Geometry Modeler

An efficient design-by-optimization procedure requires a versatile solid geometry kernel that allows a variety of structures to be constructed. Moreover, the structure needs to be parameterized so that the design space may be explored during optimization. In other words, the kernel should allow a set of parameters that define certain geometrical dimensions of the constructed structure to be treated as design variables. Changing the values of these parameters should result in the reconstruction of the geometry. As the geometry evolves through optimization, the structure must remain consistent: that is, edges, faces, or volumes cannot disappear or emerge.

In order to achieve the required versatility, the modeling framework is based on a constructive solid geometry (CSG) approach in which structures are built from primitive shapes, such as boxes, cylinders, and rectangles. Each primitive has a set of parameters that defines its dimensions, thus allowing easy parameterization. Also, Boolean operations (union or subtraction) can be performed on these primitives, allowing for the quick construction of moderately complex parameterized structures. Unfortunately, the CSG is too restrictive when it comes to more complex shapes. However, sophisticated structures can be obtained employing concepts used in the boundary representation (Brep) approach, such as rotations, mirroring, extrusions, cloning, and filleting. For this reason, the CSG in the geometry kernel has been augmented with Brep operations. Moreover, the user may introduce multilevel relative coordinate systems, all of which will considerably enhance the modeling capabilities.

To implement the geometry definition and transformation module, we used the widely known and proven open source Open CASCADE software development platform [12]. This provides procedures for geometrical computations and data exchange. The platform is actively maintained and new features, such as parallelization, are continuously added.

One of the advanced features of the geometry kernel of the framework, and one which is crucial for efficient shape optimization, is the ability to track deformations of a geometry while preserving its topological properties. During optimization, the design variables, namely the parameters defining the structure, are altered, resulting in a need to reconstruct the geometry after each change. Moreover, when gradient optimization methods are used, the sensitivities of the goal function need to be computed in each iteration, which involves several simulations of the structure with small perturbations in the parameters. The deformations are tracked each time the geometry is perturbed, and this is done in parallel for the entire set of optimization parameters. The geometry changes are bound to the mesh movements. As a result, multiple mesh generations are omitted and, instead, the mesh is generated only once per iteration. It is then modified according to the deformation data. Usually only a small part of the mesh needs to be modified; for example, some vertices might be moved. Not only does this speed up computation, but it also makes the sensitivities more accurate, effectively making gradient optimization possible.

4. Optimizer

In almost every design cycle of passive microwave components that uses an electromagnetic simulator as a response prediction tool, much effort is associated with the numerical tuning of the final high-accuracy model. This tuning may be manual or automated (that is, based on optimization). However, the selection of the proper optimization scheme for a given problem is of great importance, since the cost of the process is usually very high.

In general, optimization schemes can be divided into two groups: global and local algorithms. Global techniques allow the global minimum of the cost function to be found, and mostly use nondeterministic algorithms. Genetic algorithms, particle swarm optimization, and simulated annealing techniques belong to this group. Such techniques usually need a high number of cost-function evaluations, and are therefore not recommended for cases where a single cost-function evaluation is time consuming.

Fast optimization techniques rely on the gradients of the cost function to predict the direction of its movement in the optimization space. Gradient methods are an example of local schemes, which means that they stop when a local minimum is reached. Fortunately, this is not a problem, if the cost function has no local minima in the neighborhood of the starting point.

As full-wave optimization is time consuming, we have

decided to use gradient techniques. The basic challenge in the application of gradient optimization techniques with FEM comes from the fact that the three-dimensional finite element method uses a discrete geometry definition described by a mesh. To compute the gradient, the geometry is perturbed and the response of the structure is recalculated. The gradient can be then evaluated using the finite difference approach. At this stage, two scenarios are possible:

- remesh the geometry after its perturbation; or
- evaluate the mesh perturbation without remeshing.

The first option is easy to realize with most FEM code. However, since the perturbation is usually small for the gradient computation, the remeshing of the geometry can introduce additional errors that can affect the quality of the gradient. The perturbed problem is regenerated from scratch, and so the global FEM matrix properties also change. Additionally, for complex structures, the remeshing time can be substantial. The second option is in many ways superior: the remeshing error can be eliminated and the data generated for the unperturbed FEM problem can be reused. Since only a small number of nodes are usually affected by the perturbation arising from the change in one design variable x_i, the updates to the global FEM matrices, denoted ΔK_i and ΔM_i, are very sparse and cheap to evaluate. Once the perturbation matrices are known, the gradients can be evaluated relatively cheaply using adjoint sensitivities [14].

Mesh perturbation methods need to allow the movement of the mesh nodes with the change in geometry to be traced for arbitrary complex solids. As discussed in the previous section, this is achieved by coupling the optimization procedures to the 3D modeler used to input the problem geometry. Fig. 2 shows examples of local mesh perturbation for the complex geometries that can be found in combline filters used in base stations.

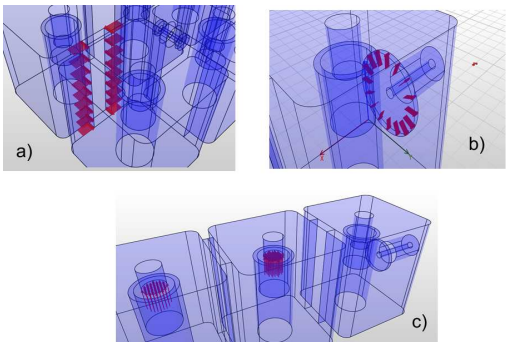

Fig. 2. Examples of mesh–node movement (red arrows) when geometry description is modified: a) iris width , b) tap–probe radius, c) tuning-screw length change.

4.1 Zero-Pole Filter Optimization of Filters and Multiplexers

The performance of the optimization strongly depends on the definition of the cost function. Since FEM is often used for complex filter and multiplexer design, we developed a cost function that is customized for this purpose. In microwave filter design, the response of the filter is usually described with a rational function defined by the positions of its zeros and poles. For many types of filters, the ideal reference response can be derived analytically, as in the case of generalized Chebyshev bandpass filters [10]. As has been shown in [15], [16], [17], in such cases, the cost function F for filter optimization can be defined using the zeros and poles of transfer functions as

$$F = \|p_r - p_o\| + \|z_r - z_o\| \tag{10}$$

where p_r and z_r are the vectors of reference zeros and poles, while p_o and z_o are the vectors of zeros and poles of the rational representation of the response of the device being optimized. The zeros and poles can be defined for the scattering parameters s_{11} or s_{21}, or for both s_{11} and s_{21}. To construct the rational model of the response from the simulated results, a direct interpolation or vector-fitting technique can be used [11].

The zero-pole-based algorithm can be generalized to multiplexer design. In this case, the return loss response of each channel filter in the channel passband can be treated as the response of a simple double-terminated filter. For example, in the case of a diplexer that has a common port number 1 and two channel outputs numbered 2 and 3, the zero-pole-based optimization can be defined using the filtering characteristics s_{22}, s_{33}, and optionally s_{21} and s_{31}. In the result, it is possible to optimize the return loss response of all channels at the same time.

5. Parallel Implementation

For optimal performance, the computational engine was designed in such a way that it can use all cores available in the workstation or server during the critical phases of simulation. All modern CPUs use multiple cores, and a new trend uses manycore architectures. The simplest parallelization strategy is to assign a separate problem to each core or processor. In this way, the problem can be solved for several frequency points or excitations concurrently. In practice, however, the number of excitation is limited and this strategy is not scalable to a larger number of cores or processors. Carrying out computations at several frequency points simultaneously can be highly efficient in terms of the utilization of CPU cores, but the RAM usage increases linearly with the number of frequency points. As RAM is crucial for solving larger problems, and the number of cores on high-end servers exceeds ten, and since fast frequency sweep can be achieved with matrix factorization at one frequency point, a parallelization strategy based on spectral decomposition does not seem to be the right way to take advantage of computer resources.

Furthermore, future generations of workstations are likely to have even more cores than are available at present.

Our assumption is that the FEM solver should be able to take advantage of both multicore and manycore processors. We therefore developed two versions, one for CPU-only architectures, and an extended version for hybrid multicore–manycore platforms. The basic version, geared towards multicore CPUs, uses OpenMP directives and libraries tuned to parallel execution for matrix generation and the computation of the projection basis needed for the fast frequency sweep technique.

The use of concurrent computations for matrix generation is particularly important in design by optimization using FEM, as the matrix needs to be generated anew at each design iteration. The impressive speed gains of this step can be achieved when one or more than one manycore platforms (e.g., graphics processing units) are available in the system. In such an environment, thousands of threads are run in parallel, leading to very efficient utilization of computational resources. As explained in [19], concurrency within one GPU is exploited at various stages. In our case all cores available on the CPU and GPUs are used [20], [21]. This task can be off-loaded entirely to a GPU if the matrix is not too large. The generation of large matrices is much more challenging. In this case, one or more GPUs are used in parallel to evaluate integrals and to assemble the fragments of a global system matrix, while the CPUs control the process, collect the submatrices furnished by GPUs, and coalesce them using all cores, working concurrently with the GPUs. Since the momory on a GPU is limited the large matrices are generated in an iterative process. In each iteration of the finite-element matrix generation, the subset of tetrahedra is processed in such a manner that batches of tetrahedra are performed in parallel (on the level of CUDA blocks); for each tetrahedron, Gaussian quadrature is parallelized (on the level of CUDA blocks); dense matrix computations (products and sums) are parallelized (on the level of CUDA threads); and concurrent streams (Hyper-Q) are assigned to each variant of the numerical integration. With double-precision arithmetic, the GPU-accelerated matrix generation of over 5 million unknowns can be carried out on a single GPU - NVIDIA Tesla K40 GPU (2880 CUDA cores, 12 GB) - in a matter of tens of seconds, as opposed to a high-end server with 2 CPUs - 2 INTEL Xeon Sandy Bridge E5-2687W (total 32 logical cores, 3.1 GHz) equipped with 128 GB RAM - that requires several minutes. According to the results of our recent reported in [21] this translates to a 13-fold speed-up

Another process in which parallelization is employed in the integrated design-by-optimization framework is the computation of gradients. This requires invoking the 3D solid modeler and computing the geometry deformation with respect to each variable. Since OpenCascade, the math library we are using in the modeler, is not thread-safe, we launch a separate process for each variable, so that the multicore architecture can be made use of. The number of processes that are launched simultaneously is equal to the number of cores.

6. Computational Examples

To demonstrate the efficiency of the proposed framework, some examples of advanced simulation and design-by-optimization are given. For all structures, we give the simulation details with the number of variables and the order of finite elements used along with the running time. We compare the results with reference data or with measured results.

6.1 Dielectric Resonator Antenna

We start with the numerical analysis of the cavity-backed dielectric resonator antenna (DRA) fed with coax line. The structure of the antenna is shown in Figure 3, and a detailed description, including all dimensions and measurement results, can be found in [22]. The cavity is partially filled with two layers of lossy dielectric materials. The mesh in the open region is truncated using an absorbing boundary condition. The antenna is a moderately complex structure, but is good example to show the performance of model order reduction on lossy problems.

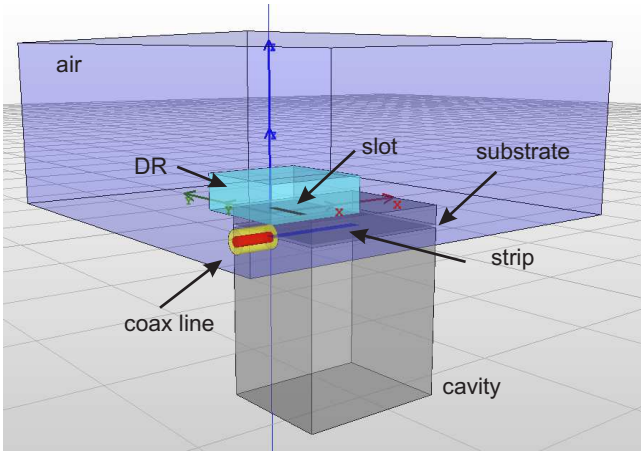

Fig. 3. Geometry of cavity-backed dielectric resonator antenna.

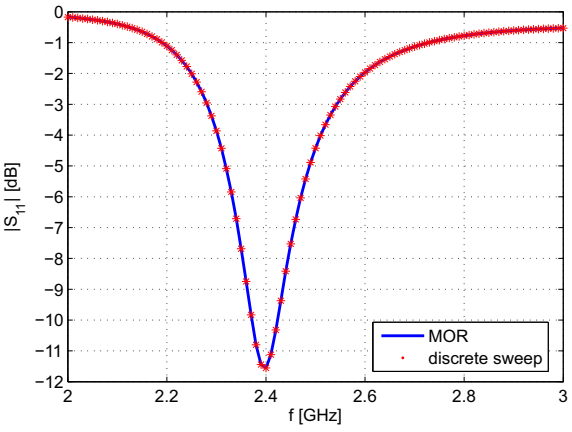

Fig. 4. Comparison of computed reflection coefficient of DRA using classical frequency sweep and MOR.

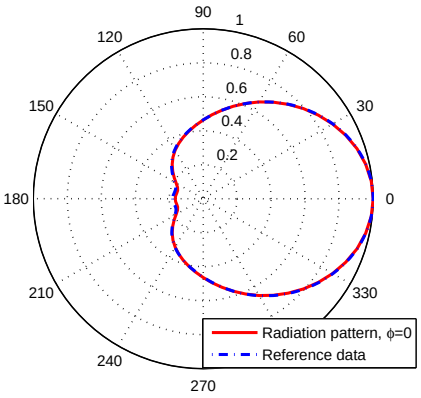

Fig. 5. Computed radiation pattern of DRA using near-to-far field transformation in the plane $\phi = 0$.

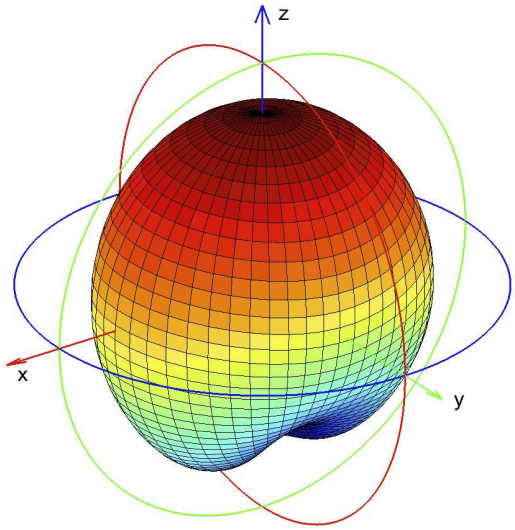

Fig. 6. Computed 3D radiation pattern of DRA using near-to-far field transformation.

A mesh of over 25000 elements was created, and applying QTCuN base functions, the resulting (complex-valued) problem involved over 659,000 unknowns. The problem was analyzed in two ways: first, using a direct solution on discrete frequency points, and secondly, by applying a model order reduction technique. The computations were carried out on a workstation equipped with a 4-core Intel i7 870 processor running at 2.93 GHz. The running time of the former simulation was 60 minutes (the solve phase was 34 seconds per frequency point), and with the application of MOR, this time was shortened to 97 s. In the second case, only a single factorization of the global finite element matrix was needed to perform the frequency sweep in the whole frequency band.

In Fig. 4, the comparison of both simulation results is shown. It can be seen that both results agree perfectly. Additionally, very good agreement with the results published in [22] is seen. Using the solution at the frequency of 2.4 GHz, the antenna radiation pattern was calculated by performing near-to-far field transformation, available within the framework. The radiation pattern shown in Fig. 5 is compared to the reference result, and once again, good accuracy can be observed. Finally, in Fig. 6, a visualization of the 3D radiation pattern of the investigated DRA is shown.

6.2 Waveguide Diplexer

The next example is a WR90 waveguide diplexer design. This device uses two eighth-order channel filters connected to a tee junction (Fig. 7). The channel passbands are 9.6 – 10 GHz and 10.2 – 10.6 GHz, with a return loss level of 20 dB. The design began from synthesized channel filters connected to the tee. In Fig. 8, the response of the initial design is shown. The structure was discretized with over 305,000 tetrahedra and second-order (LTQN) basis functions were used to construct a linear problem. This led to a problem with 2.4 million unknowns. A single simulation of the whole structure at 42 discrete frequency points, including meshing and matrix generation, took over 40 minutes. Again, a workstation with a 4-core Intel i7 870 at 2.93 GHz was used in the computations. The solve phase took about 42 seconds per frequency point.

The geometry was parameterized with 38 independent variables, defining the widths of all irises, resonator lengths, and waveguides in the junction area. With the techniques described above, we evaluated the response over the entire band and computed sensitivity with respect to all 38 variables in just 25 minutes. The optimization scheme based on the zero-pole cost function needed 21 iterations to ensure almost equiripple response in the passband. The total time taken by the optimization was 9 hours, which is one third of the time for a single iteration using a brute-force approach based on remeshing for gradient computations (The estimated time for a complete design cycle for such a suboptimal technique is about 3 weeks). The proposed framework is customizable. In this particular computational example, the optimization was carried out using a Matlab environment coupled to the 3D FEM solver and geometry kernel using COM interface API functions.

The results of the measurements of the fabricated diplexer shown in Fig. 9 indicate the excellent quality of the design. In this case, no additional tuning elements were used, and yet the simulation results are in good agreement with measurement.

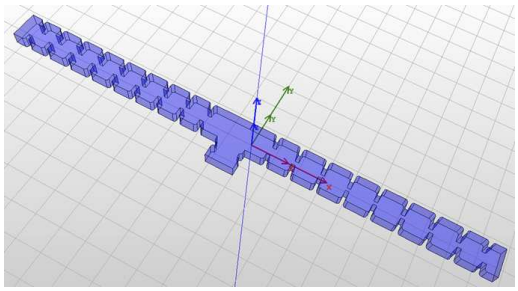

Fig. 7. Structure of waveguide diplexer.

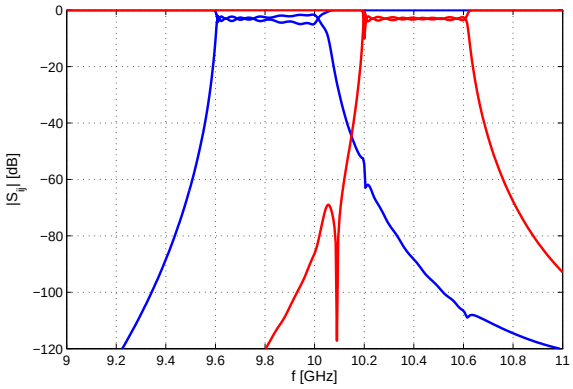

Fig. 8. Response of the initial diplexer before numerical tuning.

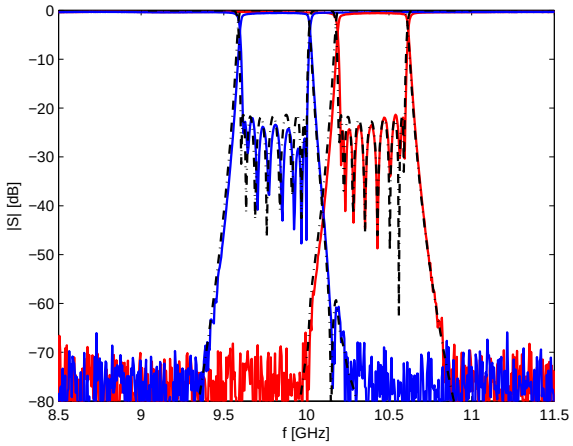

Fig. 9. Measurement of fabricated waveguide diplexer (red / blue) vs. simulation results (dashed).

6.3 Combline Diplexer

The third example is a combline diplexer on the GSM 1800 band. This is shown in Fig. 10. The channel filter passbands are set to 1710 – 1785 MHz and 1815 – 1880 MHz. In both channels, an additional cross-coupling was introduced to form a quadruplet topology and to add 2 transmission zeros to improve the selectivity of the transfer functions. The requested return loss level was set to 20 dB.

The structure was discretized with 0.53 million tetrahedral elements, which led to a linear system of equations of 3.0 million unknowns. For this problem, the running time for point-by-point frequency sweep with just 34 frequency points is 22 minutes 30 s on a dual Intel Xeon X5960 CPU server with all 12 cores engaged. This included a single-threaded mesh generation, which took about 2 minutes 30 s.

The diplexer geometry was parameterized with 32 variables, controlling tuning screws and excitation of the resonators from the coaxial line inputs. With the application of the framework described in this paper, the response of the structure with sensitivities over all parameters can be computed in only 13 minutes. In Tab. 1, a comparison of the execution times of different simulation modes is shown. It is worth noting that the overhead associated with the computation of 32 sensitivities over the MOR is just 168 seconds, or 5.25 seconds per variable. When this time is compared with the duration of direct point-by-point FEM simulation at 34 frequency points (1230 s), the overhead per variable is marginal – just 0.42%.

Simulation type	Time [s]
Direct freq. sweep (34 fp.)	1230
MOR sweep + sensitivities (32 var.)	481
MOR sweep no sensitivities	313

Tab. 1. Execution time of simulator in different modes for combline diplexer (meshing and geometry processing time not included).

To show the impact of multiple cores on the duration of the computations, we have collected in Tab. 2 the execution time for the most important stages of the simulation and the different number of threads engaged. It can be seen that the current implementation gives a significant speed-up when multicore architectures are used.

	Time [s]			
Number of threads	1	2	6	12
Matrix generation	143	66	39	34
MOR	693	370	251	220
Sensitivities	260	164	152	157
Other	111	82	74	70
Total time	1207	682	516	481

Tab. 2. Execution times of selected computational routines executed during optimization (MOR + sensitivity computation) vs. the number of threads for combline diplexer (meshing time not included).

The zero-pole-based optimization was implemented via a COM interface and needed 40 iteration to converge to the result shown in Fig. 11; the total time needed for the optimization was only 520 minutes. The progress of the optimization, shown in Fig. 12, confirms the excellent properties of the zero-pole cost function adapted for multiplexer design—starting from a poor initial response, the optimization technique converged without becoming stuck in a local minimum. The results for the running time given above and the monotonic convergence of the optimization confirm that the approach described in this paper ensures the quick computation of high-quality gradients.

To demonstrate the accuracy of the proposed design-by-optimization approach, the filter was fabricated (Fig. 13) and measured. The results shown in Fig. 14 once again show the excellent quality of the design.

7 Conclusion

In this paper, an efficient framework for the fast simulation and optimization of passive high-frequency devices through the application of the 3D finite element method has been demonstrated. Most

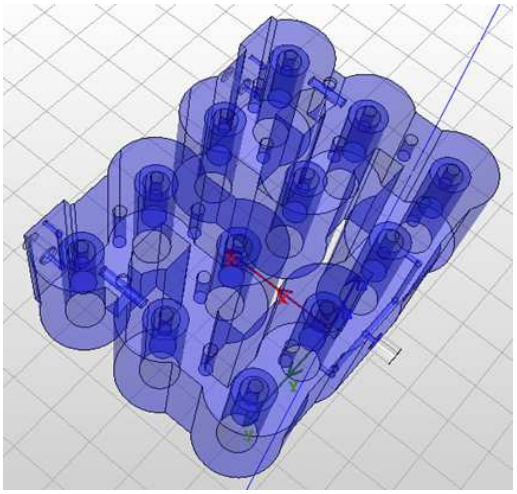

Fig. 10. Structure of combline diplexer for GSM 1800 band.

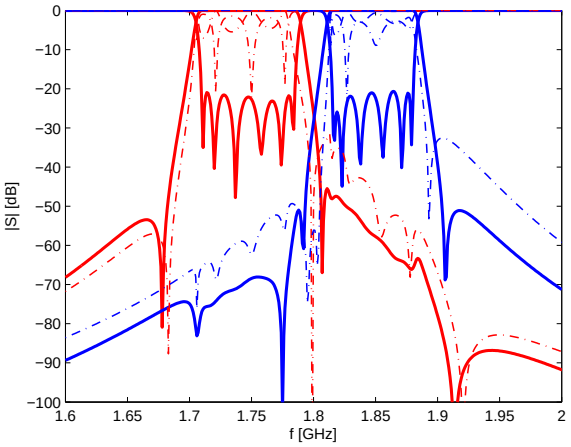

Fig. 11. Results of diplexer response before (dashed) and after (solid) numerical optimization.

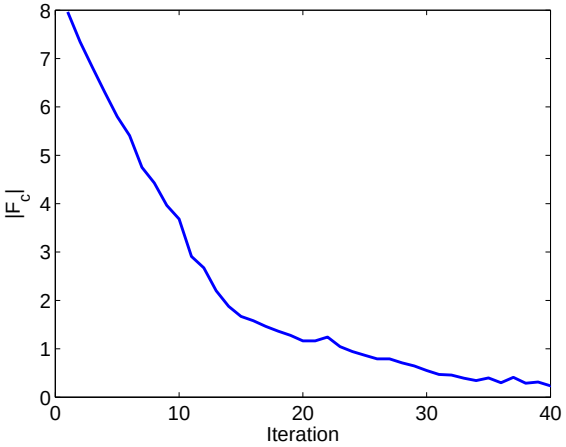

Fig. 12. Progress of optimization: values of the cost function in subsequent iterations.

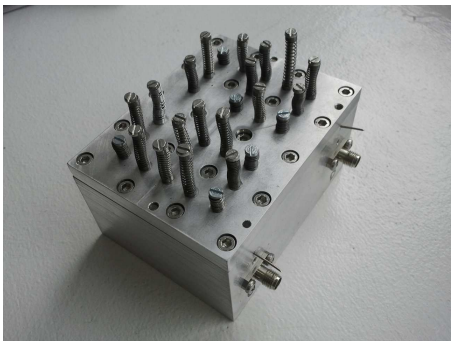

Fig. 13. Manufactured prototype of combline diplexer.

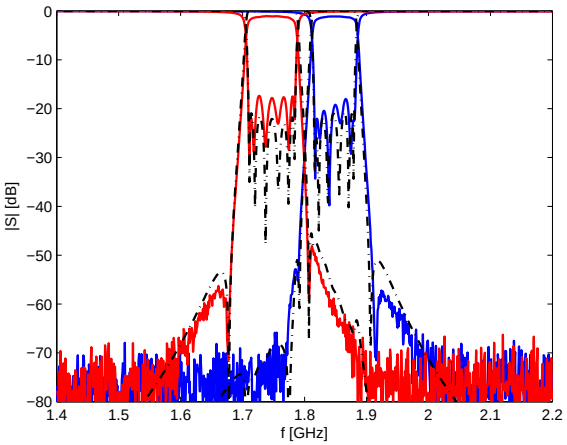

Fig. 14. Results of measurement of fabricated combline diplexer (red/blue) vs. simulation results (dashed).

concepts described in the this paper have been integrated in the software package [23], whose components can be called from Matlab using an API. This adds flexibility and allows the framework to be adapted to specific computational tasks or optimization techniques, as demonstrated in this paper for diplexer design. Details related to the running time and the size of the problems are given for the nontrivial examples of a dielectric resonator antenna with lossy dielectrics and two designs of complex microwave diplexers, in order to demonstrate the efficiency of the approach. Measurement confirms the high accuracy of the computations and the usefulness of the framework for fullwave design by optimization of complex practical circuits.

Acknowledgments

This work was supported by the Polish National Science Centre under contract 2012/07/B/ST7/01241, and by the National Centre for Research and Development under contract Lider/21/148/L-1/09/NCBiR/2010. The research related to GPU computing was carried within the WiComm's CUDA Center for Computational Electromagnetics and supported by the Gdansk University of Technology via statutory funds and by NVIDIA Inc. (Tesla C2075, Tesla K40 GPU donations from NVIDIA are gratefully acknowledged).

References

[1] RUBIO, J., ARROYO, J., ZAPATA, J. Analysis of passive microwave circuits by using a hybrid 2-D and 3-D finite element mode-matching method. *IEEE Transactions on Microwave Theory and Techniques*, 1999, vol. 47, p. 1746 - 1749.

[2] INGELSTROM, P. A new set of H(curl)-conforming hierarchical basis functions for tetrahedral meshes. *IEEE Transactions on Microwave Theory and Techniques*, 2006, Vol. 54, p. 106 - 114.

[3] SCHÖBERL, J. NETGEN An advancing front 2D/3D-mesh generator based on abstract rules. *Computing and Visualization in Science*, 1997, vol. 1, p. 41 - 52.

[4] DHAENE, T., UREEL, J., FACHE, N., DE ZUTTER, D. Adaptive frequency sampling algorithm for fast and accurate S-parameter modeling of general planar structures. In *IEEE MTT-S International Microwave Symposium Digest*. Orlando (FL, USA), 1995, p. 1427 - 143.

[5] SLONE, R. D., LEE, J.-F., LEE, R. Multipoint Galerkin asymptotic waveform evaluation. In *IEEE Antennas and Propagation Society International Symposium*. Salt Lake City (UT, USA), 2000, vol. 4, p. 2356 - 2359.

[6] SLONE, R. D., LEE, R., LEE, J.-F. Well-conditioned asymptotic waveform evaluation for finite elements. *IEEE Transactions on Antennas and Propagation*, 2003, vol. 51, no. 9, p. 2442 - 2446.

[7] DE LA RUBIA, V., RAZAFISON, U., MADAY, Y. Reliable fast frequency sweep for microwave devices via the reduced-basis method. *IEEE Transactions on Microwave Theory and Techniques*, 2009, vol. 57, no. 12, p. 2923 - 2937.

[8] ODABASIOGLU, A., CELIK, M., PILEGGI, L. T. PRIMA: passive reduced-order interconnect macromodeling algorithm. In *IEEE/ACM International Conference on Computer-Aided Design*, 1997, p. 58 - 65.

[9] SHEEHAN, B. N. ENOR: model order reduction of RLC circuits using nodal equations for efficient factorization. In *36th Design Automation Conference Proceedings*. 1999, p. 17 - 21.

[10] CAMERON, R. J. General coupling matrix synthesis methods for Chebyshev filtering functions. *IEEE Transactions on Microwave Theory and Techniques*, 1999, Vol. 47, no, 4, p. 433 - 442.

[11] GUSTAVSEN, B., SEMLYEN, A. Rational approximation of frequency domain responses by vector fitting. *IEEE Transactions on Power Delivery*, 1999, vol. 14, no. 3, p. 1052 - 1061.

[12] *Open CASCADE Technology, 3D Modeling & Numerical Simulation* [Online]. Available at: http://www.opencascade.org/

[13] BANDLER, J. W., BIERNACKI, R., CHEN, S. H., GROBELNY, P. A., HEMMERS, R. H. Space mapping technique for electromagnetic optimization. *IEEE Transactions on Microwave Theory and Techniques*, 1994, vol. 42, no. 12, p. 2536 - 2544.

[14] NIKOLOVA, N. K., ZHU, J., LI, D., BAKR, M. H., BANDLER, J. W. Sensitivity analysis of network parameters with electromagnetic frequency-domain simulators. *IEEE Transactions on Microwave Theory and Techniques*, 2006, vol. 54, no. 2, p. 670 - 681.

[15] KOZAKOWSKI, P., MROZOWSKI, M. Quadratic programming approach to coupled resonator filter CAD. *IEEE Transactions on Microwave Theory and Techniques*, 2006, vol. 54, no. 11, p. 3906 - 3913.

[16] KOZAKOWSKI, P., MROZOWSKI, M. Automated CAD of coupled resonator filters. *IEEE Microwave and Wireless Components Letters*, 2002, vol. 12, no. 12, p. 470 - 472.

[17] JEDRZEJEWSKI, A., LESZCZYNSKA, N., SZYDLOWSKI, L., MROZOWSKI, M. Zero-pole approach to computer aided design of in-line SIW filters with transmission zeros. *Progress in Electromagnetics Research*, 2012, vol. 131, p. 517 - 533.

[18] FOTYGA, G., NYKA, K., MROZOWSKI, M. Multilevel model order reduction with generalized compression of boundaries for 3-D FEM electromagnetic analysis. *Progress in Electromagnetics Research*, 2013, vol. 139, p. 743 - 759.

[19] DZIEKONSKI, A., SYPEK, P., LAMECKI, A., MROZOWSKI, M. Finite element matrix generation on a GPU. *Progress in Electromagnetics Research*, 2012, vol. 128, p. 249 - 265.

[20] DZIEKONSKI, A., SYPEK, P., LAMECKI, A., MROZOWSKI, M. Generation of large finite-element matrices on multiple graphics processors. *International Journal for Numerical Methods in Engineering*, 2013, vol. 94, no. 2, p. 204 - 220.

[21] DZIEKONSKI, A., SYPEK, P., LAMECKI, A., MROZOWSKI, M. GPU-accelerated finite-element matrix generation for lossless, lossy, and tensor Media. *IEEE Antennas and Propagation Magazine*, 2014 (in print).

[22] BOROWIEC, R. , KUCHARSKI, A. A. , SLOBODZIAN, P. M. Slot excited dielectric resonator antenna above a cavity analysis and experiment. In *XVI International Conference on Microwaves, Radar and Wireless Communications (MIKON)*. Krakow (Poland), 2006, vol. 2, p. 824 - 827.

[23] *eminvent.com - InventSim* [Online]. Available at: http:// www.eminvent.com

About Authors ...

Adam LAMECKI received his M.Sc. and Ph.D. (with honors) degrees in microwave engineering from Gdańsk University of Technology (GUT), Gdańsk, Poland, in 2002 and 2007, respectively. He was the recipient of a Domestic Grant for Young Scientists awarded by the by Foundation for Polish Science in 2006. In 2008, he received the Prime Minister's Award for his doctoral thesis and, in 2011, a scholarship from the Ministry of Science and Higher Education. His research interests include surrogate models and their application in the CAD of microwave devices, computational electromagnetics (mainly focused on the finite element method), and filter design and optimization techniques.

Lukasz BALEWSKI received his M.Sc. and Ph.D. (with honors) degrees in microwave engineering from Gdańsk University of Technology (GUT), Gdańsk, Poland, in 2003 and 2008, respectively. His research interests include CAD of microwave devices, filter design, and optimization techniques. He is the coauthor of several software tools for microwave filter design.

Michal MROZOWSKI received his M.Sc. and Ph.D. degrees, both with honors, from Gdańsk University of Technology in 1983 and 1990, respectively. In 1986, he joined the Faculty of Electronics, Gdańsk University of Technology, where he is now a Full Professor, Head of the Department of Microwave and Antenna Engineering, Director of the Center of Excellence for Wireless Communication Engineering (WiComm), and Head of the NVIDIA CUDA Research Center for Computational Electromagnetics. He is a Fellow of IEEE.